As part of an EU program to support protected areas in Chad, it has been demonstrated that Sentinel data produced by the European Union's Copernicus program makes it possible to calculate an indicator of "**change of habitat**". This anthropogenic indicator is detected through several biogeophysical indicators such as the change in vegetation cover, water surfaces, ploughing, savanna fires, traces of transhumance ...

Surveillance was tested here using two successive acquisitions of Sentinel-2 data (High Resolution optical or HR) and Sentinel-1 (HR radar) in Ouadi-Rimé Ouadi-Achim, the largest reserve. It may also be necessary to access meteorological data and in particular precipitation data which are also available free of charge. Sentinel-1 and Sentinel-2 products have a pixel size of 10 meters. It is shown that changes of a few pixels can be detected, that is, surfaces much smaller than the required 0.5 ha.

The photo-interpretation of the satellite images of this pre-study was carried out without knowledge of the field. A more detailed analysis will have to be validated with the Chadian observers and technicians themselves.

Support to protected areas

Ouadi-Rimé Ouadi-Achim Reserve (Chad)

2D_layer_stack

Sentinel-2 (optical HR)

For each of the 2 optical satellites S2A and S2B, the cycle time is 10 days. If both are active, the cycle time is 5 days. The next S2C and S2D satellites will be launched in the next 2 to 3 years. If they are active, we can get a revisit time of 2.5 days.

The difference (fig.1b) between the tile observed on November 17 (fig.1d) and that of November 7 (fig.1c) is calculated by a normalized difference index (NDI). This difference is photo interpreted in the following.

Fig.1: Location of the 2 reserves (a) Sentinel-2 difference (b) between the 17 (d) and 7 (c) November 2019. 2D_animation

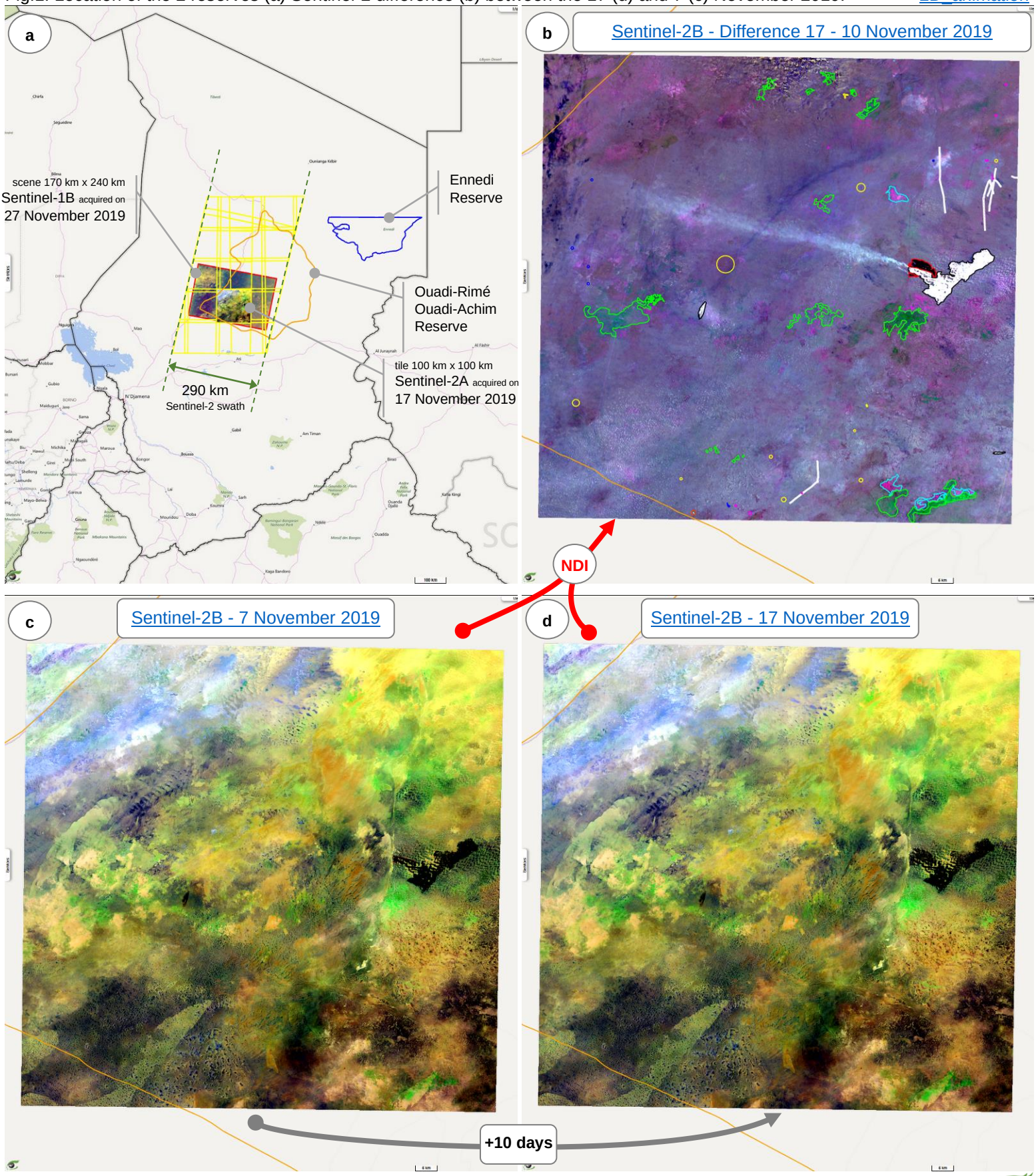

One may observe several active fires (fig.2d) on November 7, 2019 which are extinguished 10 days later (fig.2b). The flames from these active lights are clearly visible using the mid-infrared bands (bands 11 and 12) of the Sentinel-2 MSI instrument.

It is possible (to be verified) that these bush fires were initiated by the shepherds to allow the herds to graze the young shoots.

Photo-interpretation of the NDI (Normalized Difference Index) image (fig.2b):

1. No event - When no change is detected between the 2 dates, the area remains gray.
2. Active fires - the past active light pixels are cyan (complementary to red).
3. New burned area - the burned areas appearing only in the new image are black.
4. Old burned area - areas already burned see the ashes scattered or assimilated by the ground and the young sprouts saturate the difference in white.

Indicator 1 – Fires and burnt areas with assimilation of ashes

Fig.2: VHR image (a) and difference (b) between Sentinel-2 observed on 17 (d) and 7 (c) November 2019. 2D_animation

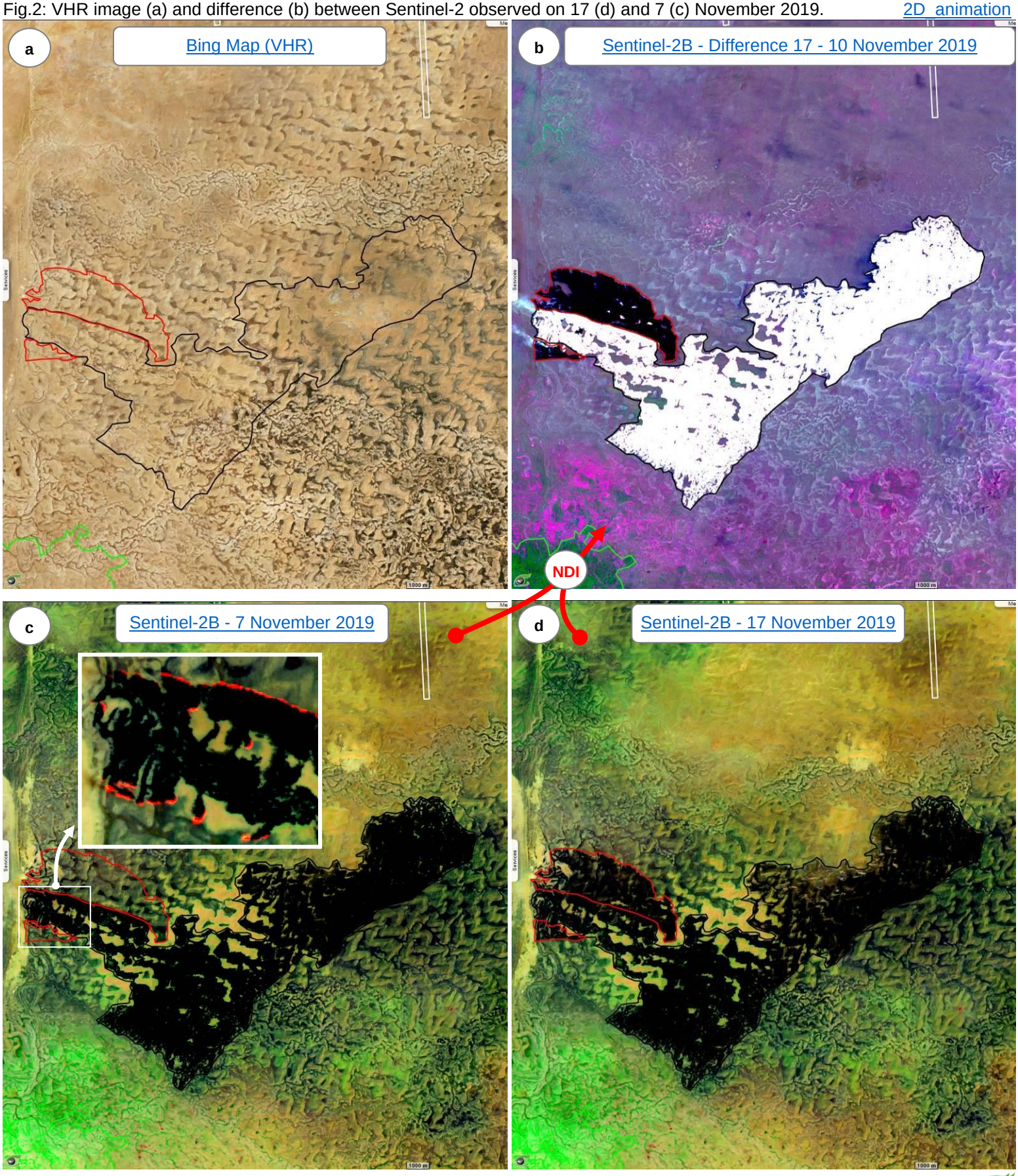

One of the advantages of the NDI normalised differences (fig.3b) is to be able to detect small differences within zones of low intensity (fig.3c and fig.3d).

We note here the plume of a burnt past area (i.e. resulting from a bush fire that took place before November 7, 2019) and coming from a "meeting point" (fig.3a). We call "meeting point" a zone of convergence of tracks (radial configuration) without permanent habitat identifiable in the Very High Resolution image (fig.3a).

Unless taking the risk of burning the inhabited part of the "meeting point", it is likely that this bush fire was accidental.

As in fig. 2, this white area shows the dispersion of the ashes or their assimilation by the soil as well as the reconquest of the soil by thin vegetation.

Unintentional fire from a “meeting point” ?

Fig.3: VHR image (a) and difference (b) between Sentinel-2 observed on 17 (d) and 7 (c) November 2019. 2D_animation

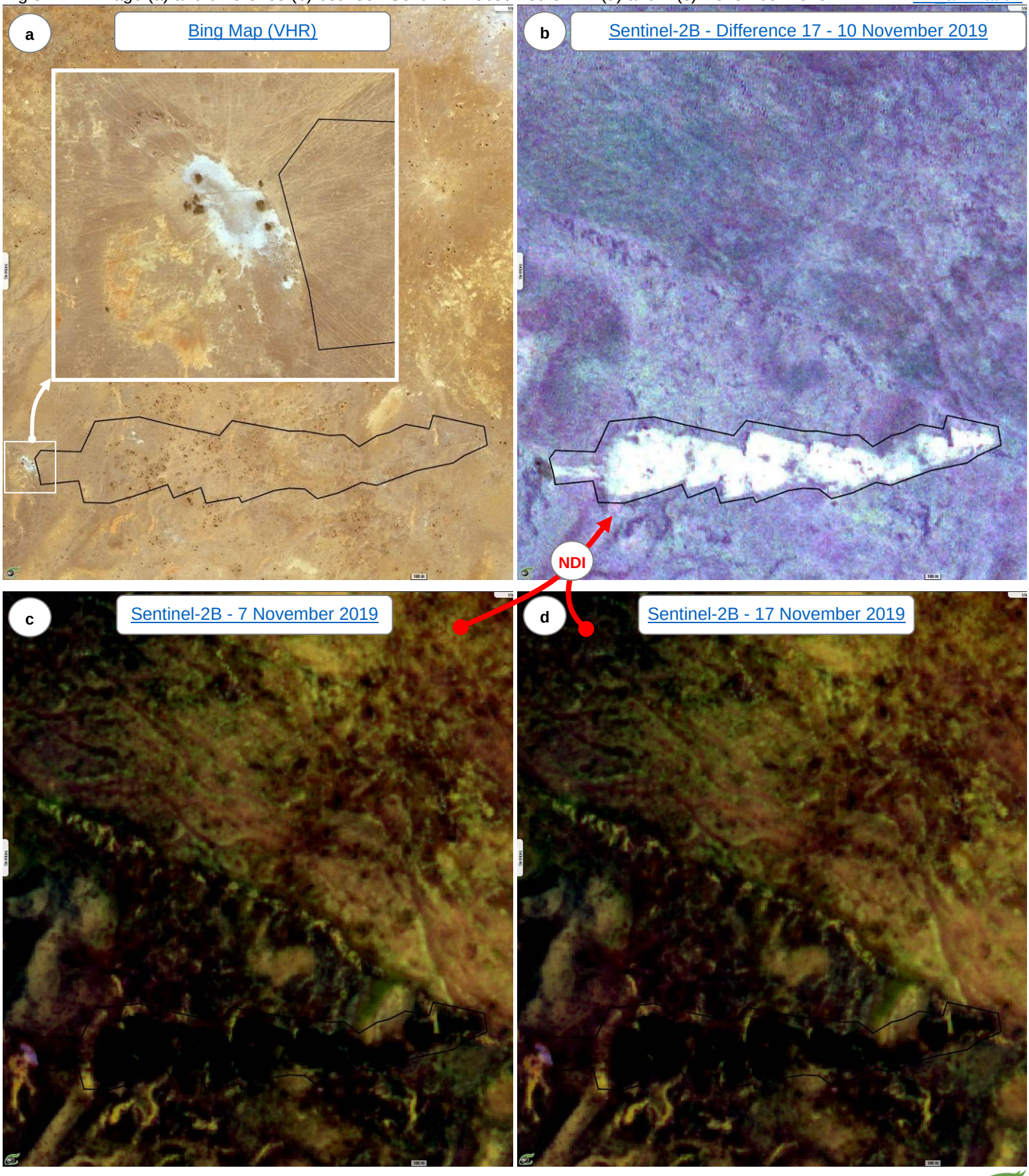

Even in desert areas (fig.4a), the few rains that occurred during the 10 days and especially the humidity (see fig.16 and fig.17) produced an increase in chlorophyll activity to which band 8 (near-infrared) of the Sentinel-2 MSI instrument is sensitive. This band is assigned to the green plane in the coloured composition 11-8-2 (RGB). This (re)vegetation is therefore marked with a bright green in fig.4b delimited with a green polygon. Conversely, a loss of vegetation appears in magenta (complementary colour of the green). These areas of devegetation have been outlined with cyan polygons.

This indicator is fundamentally linked to precipitation and soil absorption properties. The distribution of revegetation / devegetation zones are essential indices for characterizing the zones of charge / discharge of groundwater aquifers.

Variations in this index can also be correlated with agricultural activity: crops producing revegetation while harvest / ploughing producing devegetation (see next fig. 5).

Finally, we note here that the devegetated areas are systematically located immediately north of the revegetated areas. Would this not be the mark of grazing of the herds whose traces we can guess from south to north?

Indicator 2 - Revegetation / Devegetation

Fig.4: VHR image (a) and difference (b) between Sentinel-2 observed on 17 (d) and 7 (c) November 2019. 2D_animation

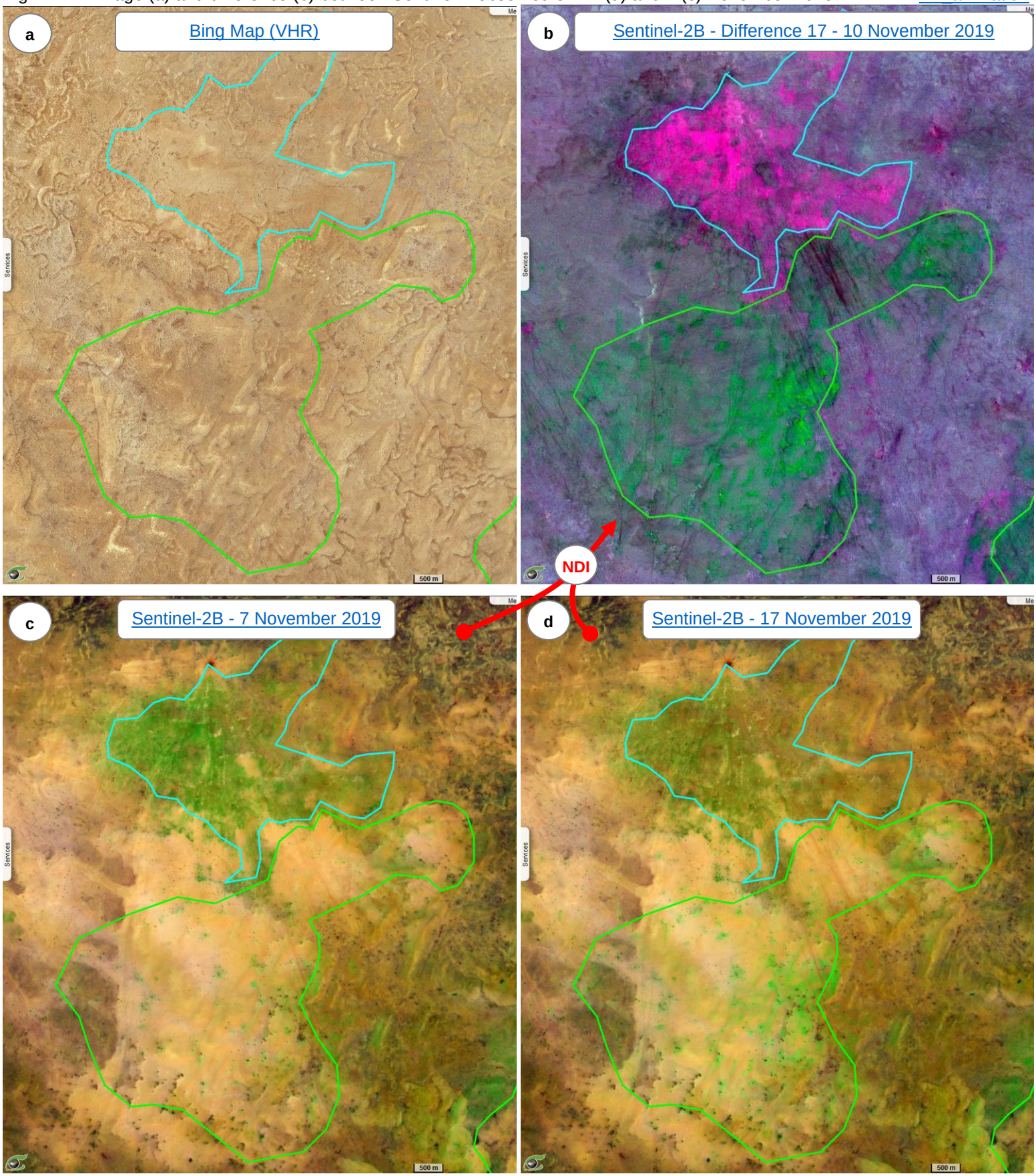

Sedentary crops are found in areas near rivers and water points. The analysis of the normalized differences (fig.5b) makes it possible to distinguish the parts of vegetation growth (in green) and the parts of sampling / harvests in the complementary colour (magenta).

We can also sometimes distinguish irrigation lines.

This indicator 2 based on the normalized difference of the bands 11,8,2 gives results very comparable to those provided by indicator 3 of NDVI (see fig.6 after).

Indicator 2 – Agricultural activities of revegetation / harvests

Fig.5: VHR image (a) and difference (b) between Sentinel-2 observed on 17 (d) and 7 (c) November 2019. 2D_animation

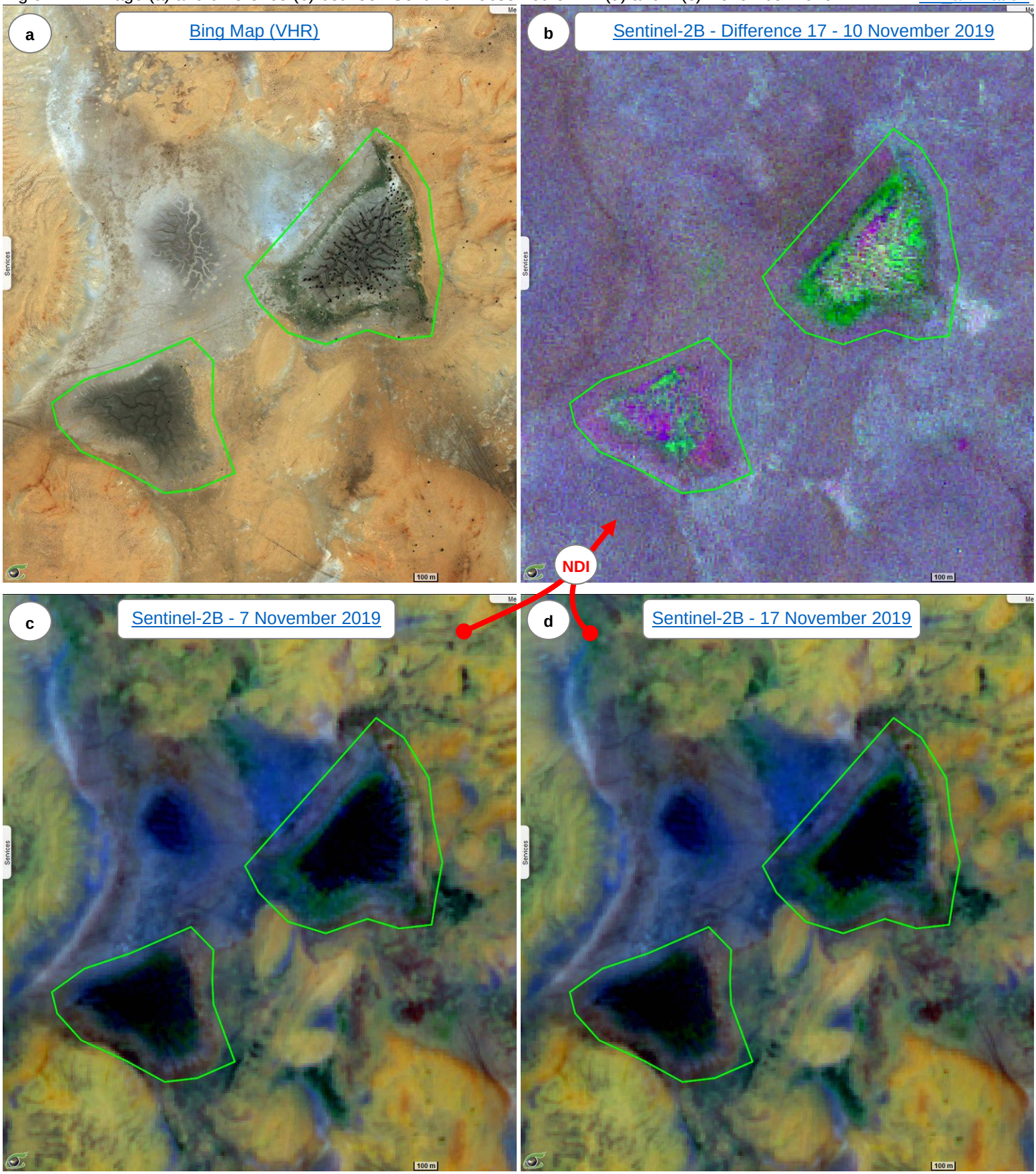

The vegetation index is probably the best known of the standardized difference indicators. Its basic version calculates the radio (NIR - Red) / (NIR + Red) where NIR is near-infrared (band 8 at 10 meters or 8A at 20 meters in the Sentinel-2 MSI instrument). Variants exist which avoid confusion sometimes encountered on bare soils.

In this arid region of Chad, the NDVI is stretched to extreme values [0; 0.25] to be able to distinguish the rare traces of vegetation. Fig.5c and fig.5d illustrate the on-the-fly computation of this NDVI using a lookup table ("NDVI LUT") highlighting the vegetation parts in green colour and the more mineral parts or water bodies in red.

The variations in this vegetation index between the two dates are also calculated on-the-fly by a difference of the two NDVIs (fig.6b). The gain of NDVI is restored in red while the loss is restored in blue using another lookup table ("polar LUT").

Indicator 3 - Gain / loss of vegetation index

Fig.6: VHR image (a) and difference (b) between Sentinel-2 observed on 17 (d) and 7 (c) November 2019. 2D_animation

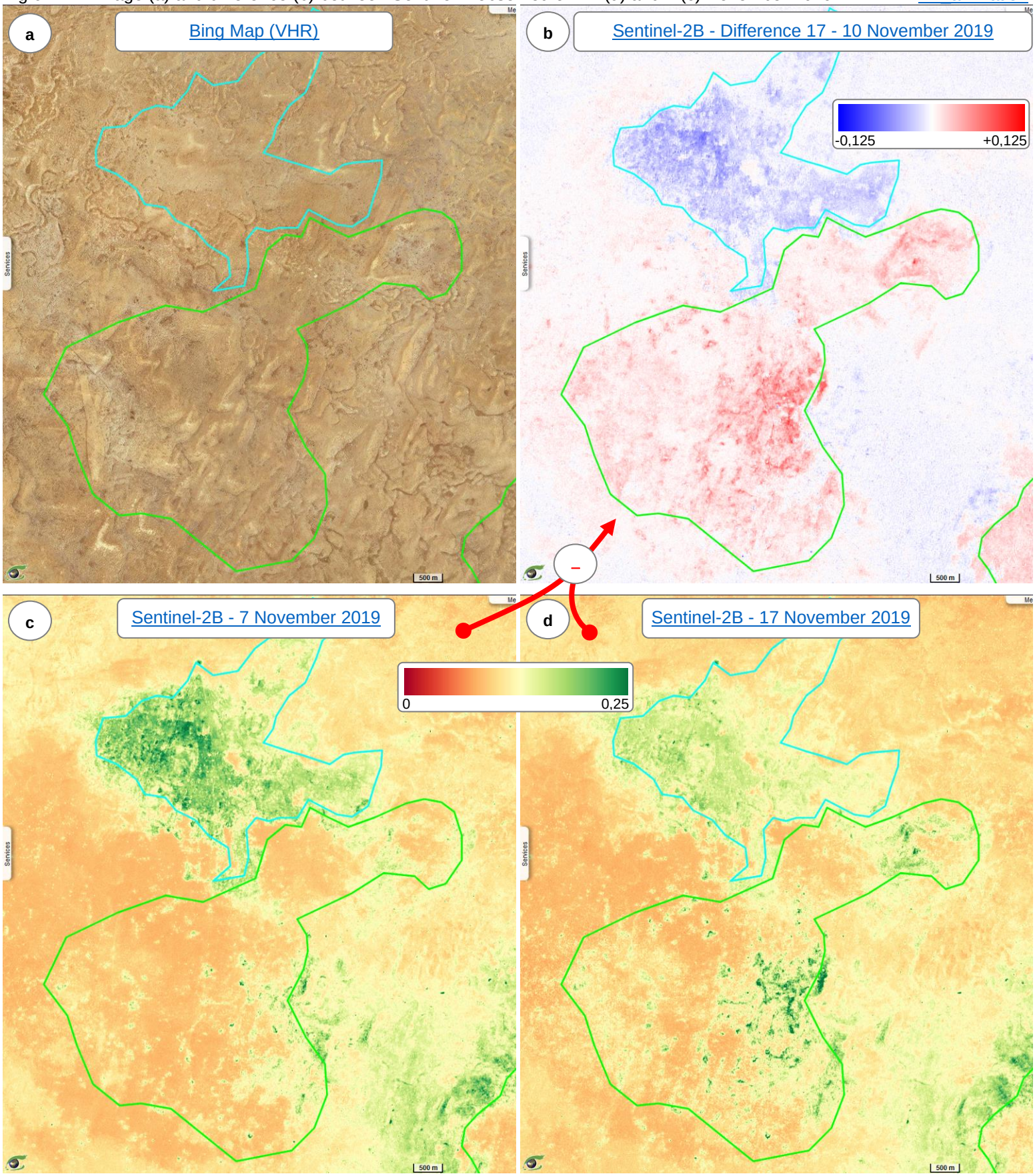

Following the scattered rains, a body of water appeared in the image of November 17, 2019 (fig.7d) when it did not appear 10 days before (fig.7c).

It is equally surprising to note that the THR image (fig. 7a) does not show a wadi shape or even any stigma of old water flow or station.

It is likely that the nomadic populations know these places of stagnation of water. It should be noted that one of the supposed transhumance routes (see fig.14) passes less than 1500 meters east of this new water point.

The near real-time warning of these new water points could be addressed to nomadic populations.

Indicator 4 – Water surfaces / New water point

Fig.7: VHR image (a) and difference (b) between Sentinel-2 observed on 17 (d) and 7 (c) November 2019. 2D_animation

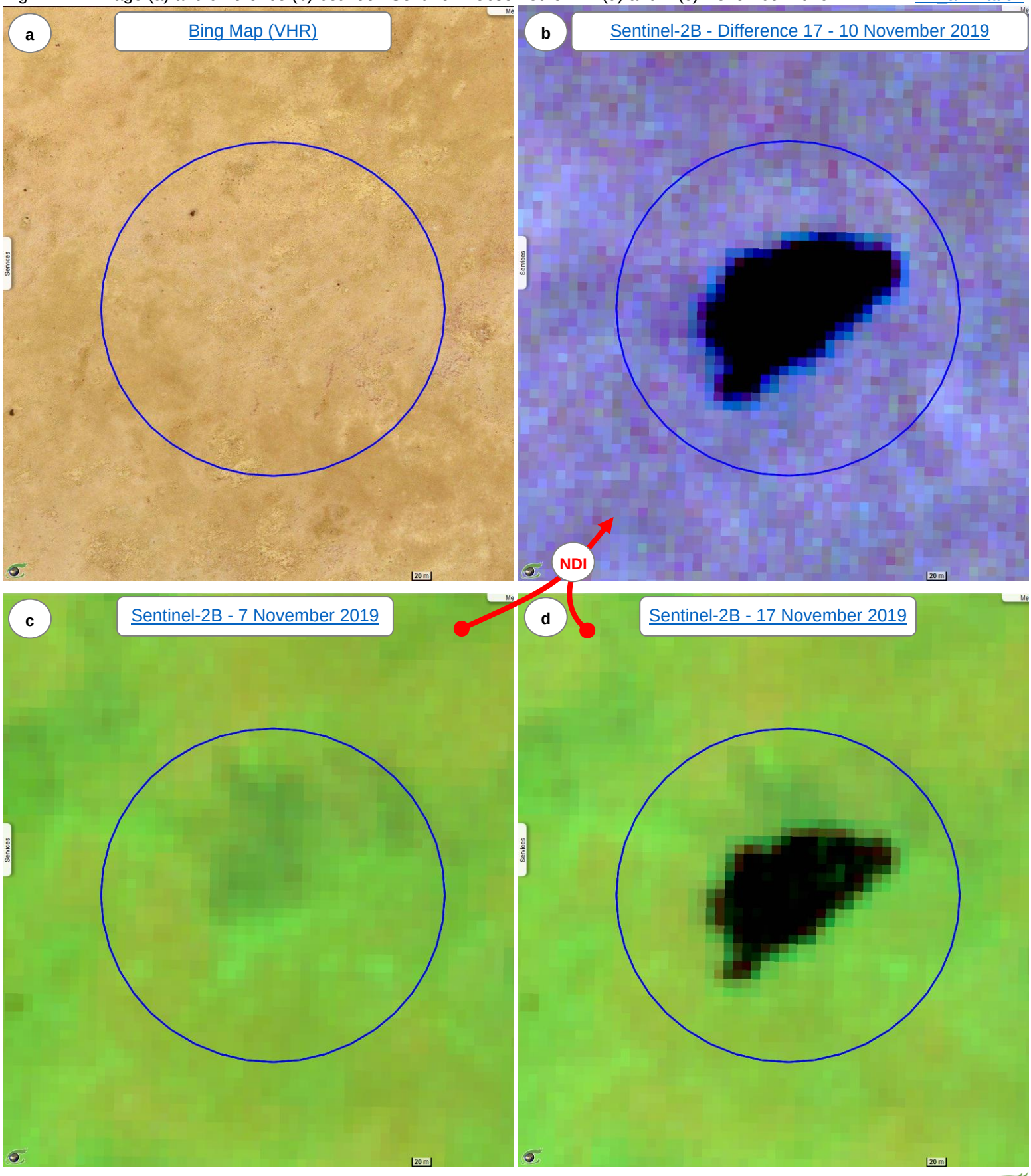

This standard difference technique also makes it possible to detect the return of water to already known oases. Fig.8a shows a zone of convergence of the tracks, a sedentary habitat and traces of wet bare soil.

The slight gain in retained water between the two dates of November 7 (fig.8c) and November 17, 2019 (fig.8d), just 10 days apart, is clearly revealed in fig.8b of normalized difference.

The position of the "water pixels" (here in the form of a crescent) makes it possible to locate with precision (pixel of 10m x 10m) the position of the reservoirs and undoubtedly to deduce the permeability in the subsurface.

Indicator 4 – Water surfaces / Oases

Fig.8: VHR image (a) and difference (b) between Sentinel-2 observed on 17 (d) and 7 (c) November 2019. 2D_animation

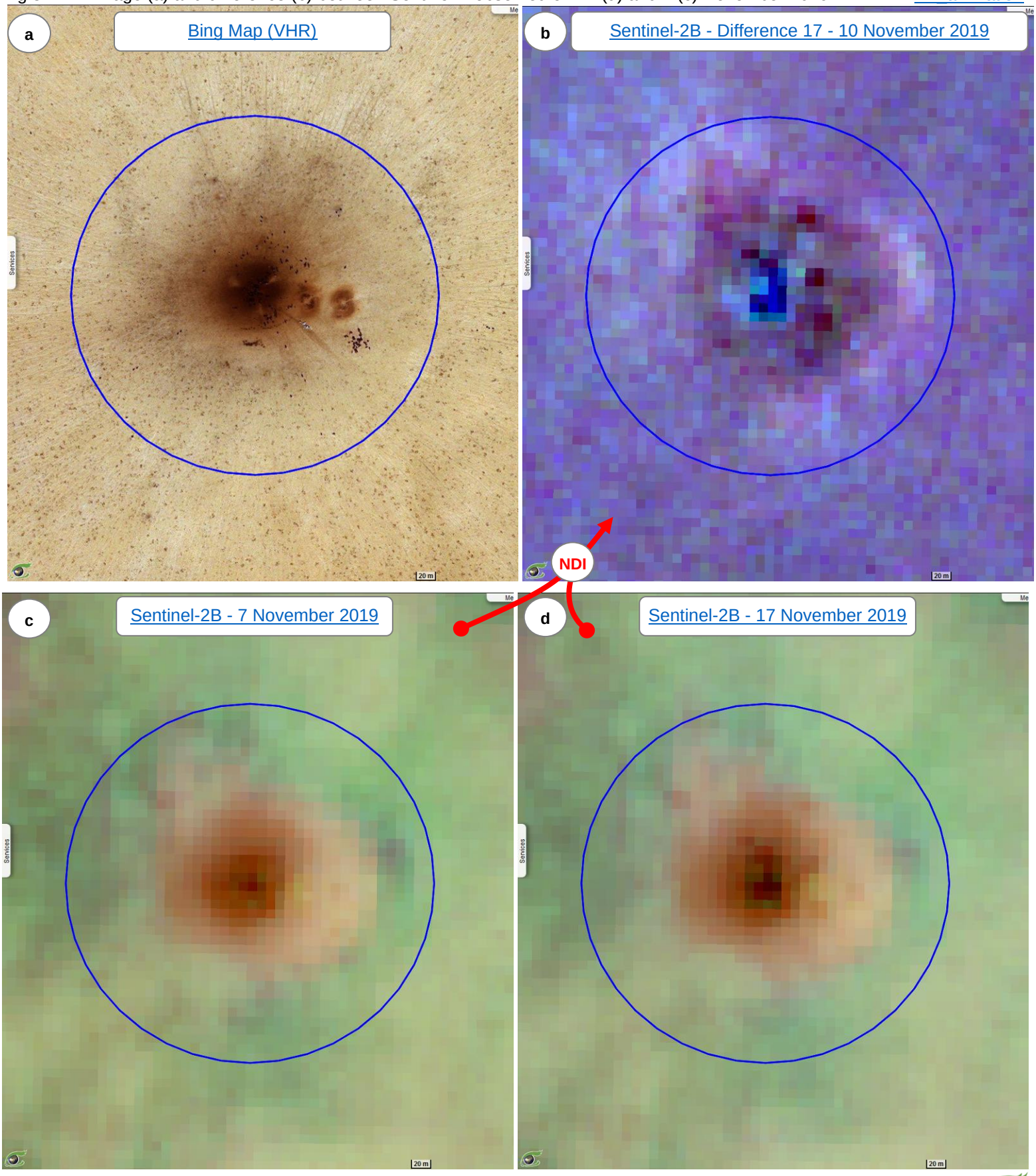

Unlike fig.7 and fig.8, we can observe a decrease in the blue component between the two dates. It is therefore yellow (colour complementary to blue) which appears in the normalized difference images.

These yellow points and surfaces appear on the dry soils or along the dry wadi or in the foothills of the hills at the interface between the sands and the rocks (fig. 9b).

The VHR image (fig. 9a) shows that the differences in water content are very dependent on the nature of the soils (surface lithology).

Indicator 4 – Water surfaces / Drying / Dewatering

Fig.9: VHR image (a) and difference (b) between Sentinel-2 observed on 17 (d) and 7 (c) November 2019. 2D_animation

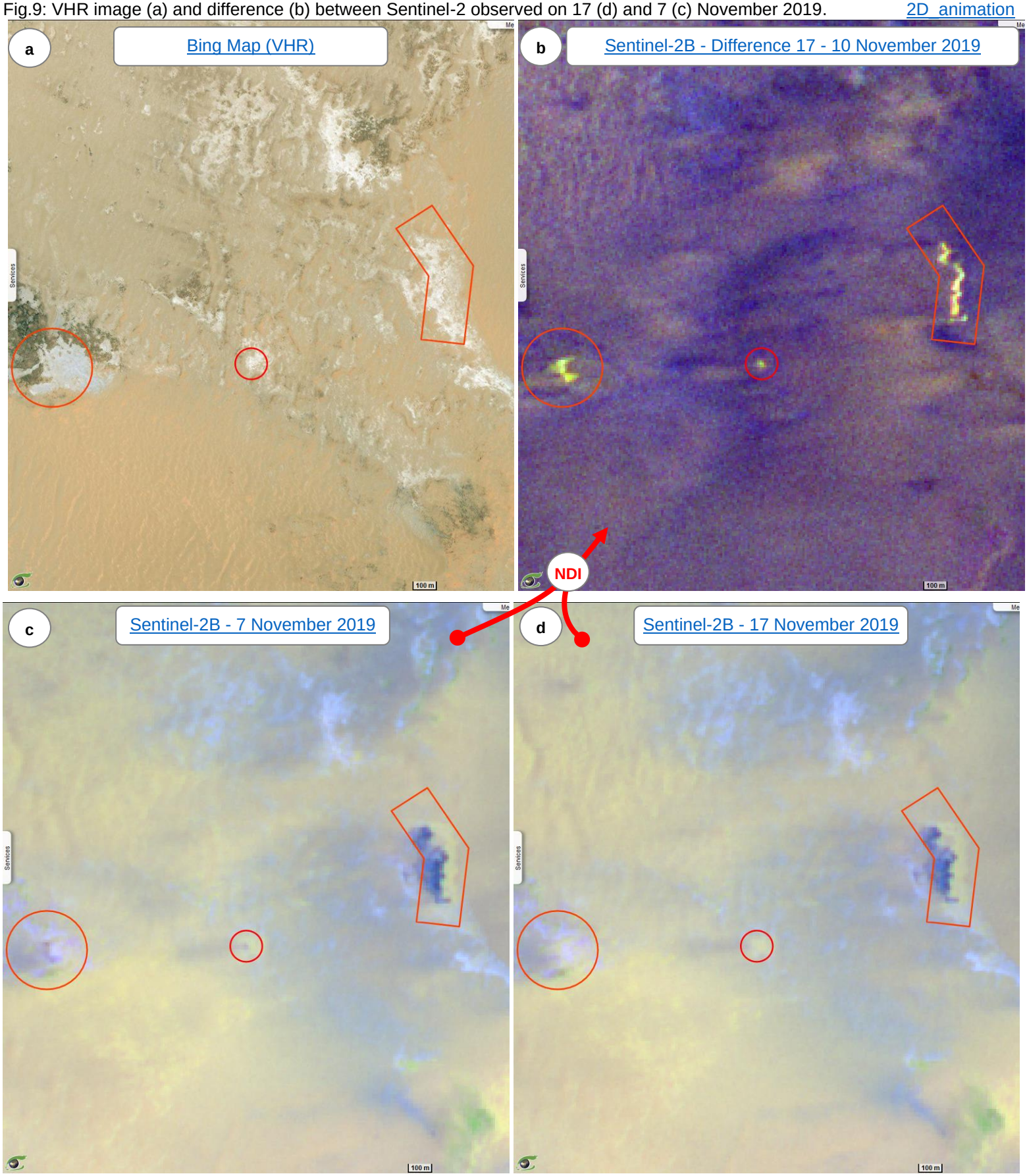

In multispectral images such as Sentinel-2 MSI, we can evaluate a “surface moisture index” by calculating a normalized difference indicator between the near-infrared band (bands 8 at 10m or 8A at 20m for Sentinel-2) and the first medium-infrared band (band 11 for Sentinel-2). The zone chosen is exactly that of fig.7 which had made it possible to identify a new water point using indicator 4.

In fig.10c and fig.10d we use a rendering table ("dry/wet LUT") to render the dry parts in brown and the wet areas in blue. As for indicator 4, there is a clear difference in values between the two dates (fig.10c and fig.10d).

This difference is illustrated in fig.10b using another rendering table ("polar LUT") showing in blue the humidity losses on November 17 and in red the humidity gains. This difference is more complex to interpret: the increase in humidity on November 17, 2019 is located around the perimeter of the area (red corolla) while the inside of the form marks a drop in the surface moisture index (blue colour). This singularity is the mark of free water revealed by index n°6 of free water (see next indicator in fig.11b).

Indicator 5 – Surface moisture index
(NIR - SWIR)

Fig.10: VHR image (a) and difference (b) between Sentinel-2 observed on 17 (d) and 7 (c) November 2019. 2D_animation

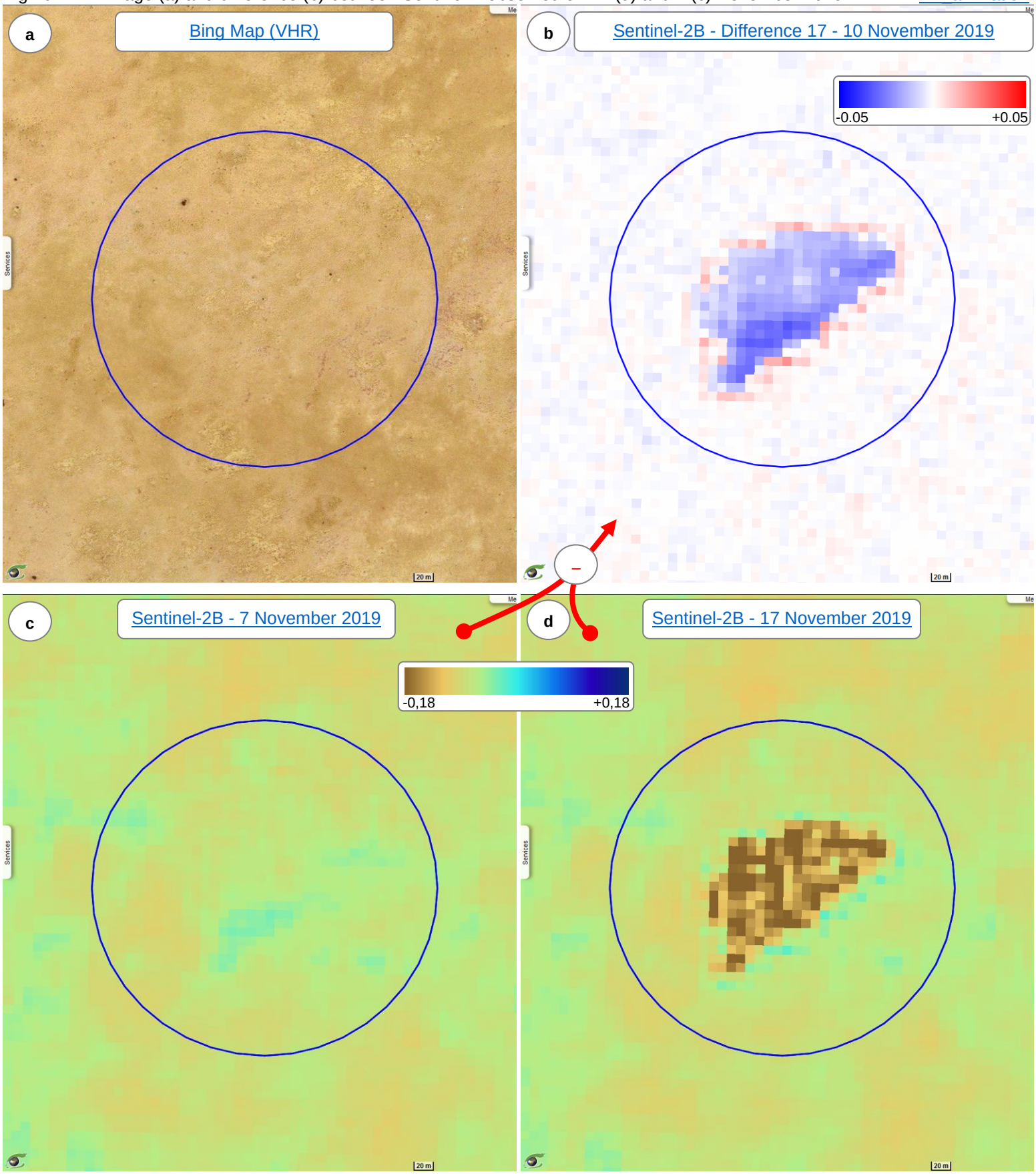

In multispectral images such as Sentinel-2 MSI, one can assess a “open water index”, that is to say of water covers and not only wet surfaces, by calculating a normalized difference indicator between the band green (band 3 to 10m for Sentinel-2) and the near-infrared band (band 8 at 10m or band 8A at 20m for Sentinel 2).

In this arid region, this index must be particularly stretched to identify very rare and small areas of open water. Here, we use the “dry / wet LUT” rendering table in which the dry zones appear in brown and the wet zones in blue.

Image of fig.11b uses the "polar LUT" rendering table to illustrate the humidity losses on November 17, 2019 by the blue colour and the free water gains by the red colour. A pattern of free water appears clearly in fig. 11b.

Thus, the new water place absent on November 7, 2019 and appearing on November 17, 2019 which had been identified by indicator n°4 (fig.7) as well as by indicator n°5 (fig.10) is confirmed by using this indicator n°6 (fig.11).

Indicator 6 – Open water index

(Green - NIR)

Fig.11: VHR image (a) and difference (b) between Sentinel-2 observed on 17 (d) and 7 (c) November 2019. 2D_animation

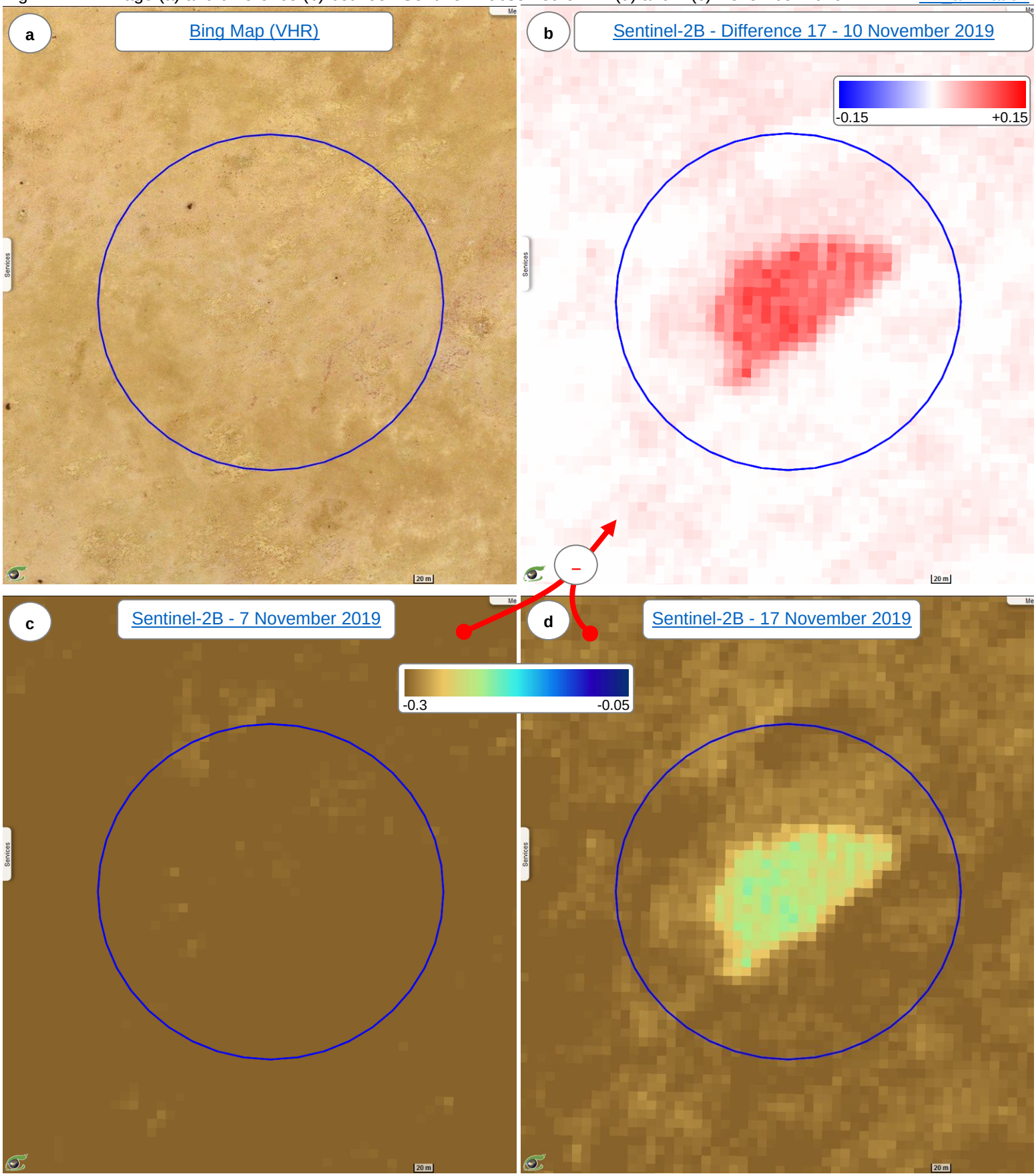

This fig.12 brings together 4 cases of human concentrations in the form of villages (very rare hard-built buildings are observed in the VHR image), oasis (case already observed with indicator n°4 of water surfaces, see fig.8) and more generally meeting points at the confluence of the tracks.

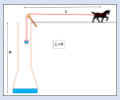

Fig.12.a1 and fig.12.a4 - "4-leaf clovers" visible in the THR images corresponding to "pastoral wells". Dark areas are due to droppings from herds waiting to drink and light areas (limits of clover petals) correspond to the animal's dewatering path (source B. Collignon, 2022).

Fig.12.a2 - probably an oil well to the north and a zone of human convergence to the south. Permanent buildings can be distinguished in the VHR image. They are located exactly between the well and the human convergence zone.

Fig. 12.a3 - village / relay along the track / road leading from the town of Ati in the south to Olanga in the north. Although this relay does not appear in the VHR image, there are many changes between the image of November 7, 2019 (fig.12.c3) and that of November 17, 2019 in which the dark bare soils marks have almost completely disappeared, reflecting more intense human activity before Nov. 7, 2019.

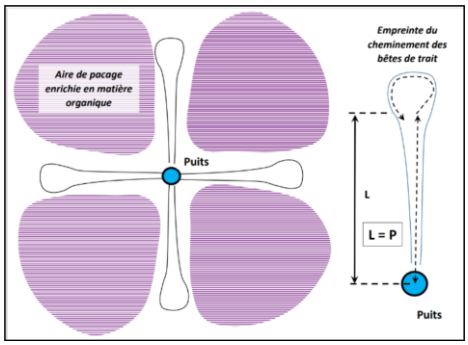

Indicator 7 - meeting points

pastoral wells, oases, drilling…

Fig.12: VHR image (a) and difference (b) between Sentinel-2 on 17 (d) and on 7 (c) Nov. 2019. anim1 anim2 anim3 anim4

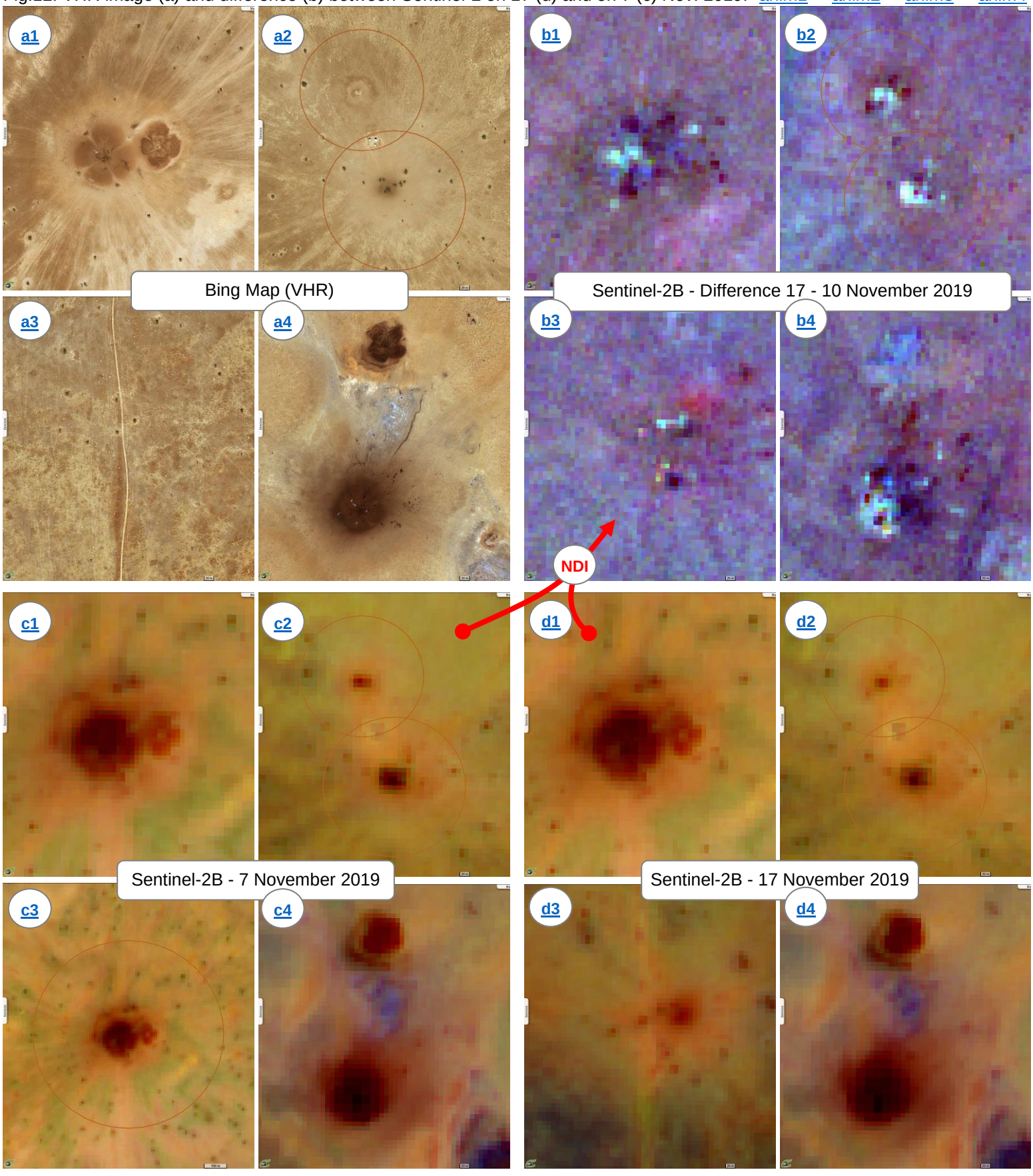

powered by VisioTerra

We can note strong variations in one part of the desert, far from roads and tracks. These high frequency variations are certainly due to human activity. The bright segment northeast of the image in fig.13b could be a small airport. Parts seem fixed (are they buildings?). We assume a movement of dark spots (signs of human activity) of about 60m towards the southwest.

These activities seem too important to be of the traditional nomadic type and are more similar to activities in heavier equipment such as in the context of mining campaigns or military activities.

Indicator 8 – Nomadic / mining / military activity?

Fig.13: VHR image (a) and difference (b) between Sentinel-2 observed on 17 (d) and 7 (c) November 2019. 2D_animation

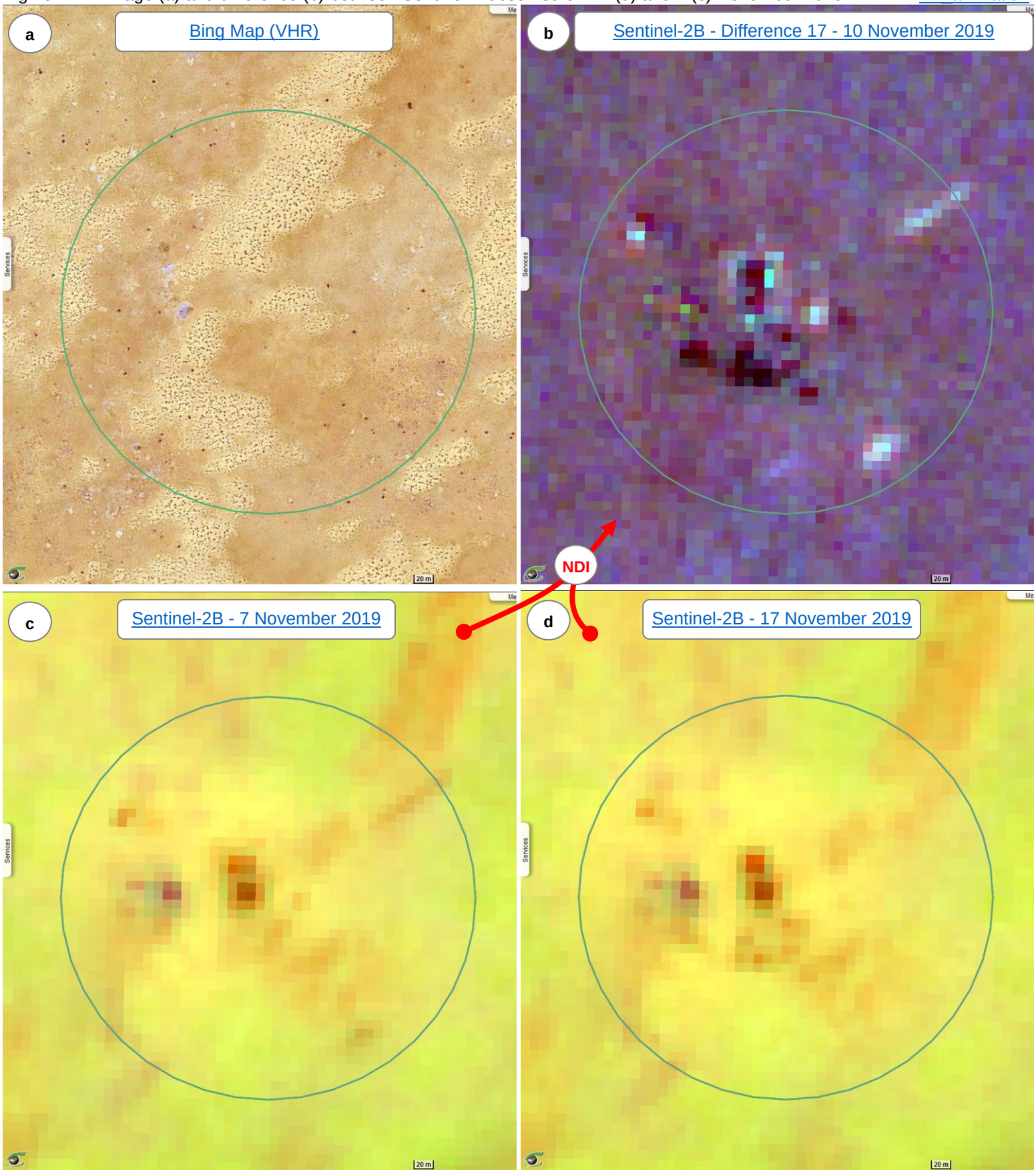

The indicator using the normalized differences makes it possible to detect variations between the two images of November 7 and 17, 2019 that are invisible to the eye. This detection operates both in very dark areas and in bright areas. Fig.14b shows for example a beam of north-south tracks rendered by a gain in blue band. A treatment with more contrast is embedded in the image to better distinguish the tracks.

This increase in the blue stripe usually indicates an increase in humidity and may be due to the trace of hooves on a wet track or due to the dispersion of lighter dust (hypotheses to be confirmed).

These traces of tracks are most certainly caused by movements of herds during transhumance or sales in some marketplaces.

Indicator 9 - Travel by roads and tracks
Probable transhumances

Fig.14: VHR image (a) and difference (b) between Sentinel-2 observed on 17 (d) and 7 (c) November 2019. 2D_animation

A great deal of data is available free of charge on the Web. Sentinel data is the main input for Copernicus services (marine, land, atmosphere, climate, emergencies and security). The first five are public.

- **CMEMS** Copernicus Maritime Environment Monitoring Service
- **CLMS** Copernicus Land Monitoring Service
- **CAMS** Copernicus Atmosphere Monitoring Service
- **C3S** Copernicus Climate Change Service
- **CEMS** Copernicus Emergency Management Service
- **CSS** Copernicus Security Service

Precipitation data are also provided by the space agencies of the United States (NASA) and Japan (JAXA).

Fig.15, fig.16 and fig.17 analyse the temperature, water vapour column and precipitation over the whole of Chad and in particular in the Ouadi-Rimé Ouadi-Achim Reserve (orange polygon). Air temperature and water vapour column data are produced by the ECMWF models every 6 hours. The date that has been chosen (6:00 GMT) is the closest one to the acquisition of the Sentinel-2 images that are the subject of this study. Low precipitation is observed around the northwest of the Reserve. These produced a drop in temperature with around 1 day difference and a significant increase in air humidity three days later.

Fig.18 shows the precipitation cycle provided by the NASA/GPM model in the rectangular area delimiting the Reserve.

Copernicus Services / NASA / JAXA

Meteorological data and precipitations

Fig.15 : Surface temperature at 6:00 GMT

+15°C +30°C 2D_animation

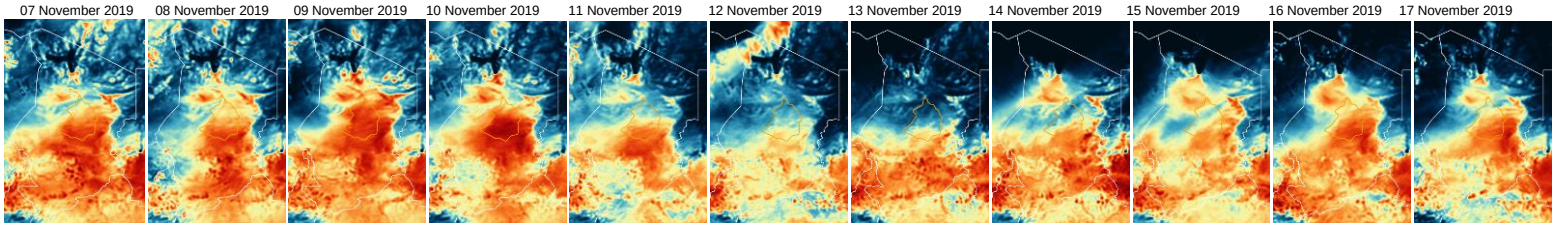

Fig.16 : Water vapour column at 6:00 GMT

0 kg/m² 30 kg/m² 2D_animation

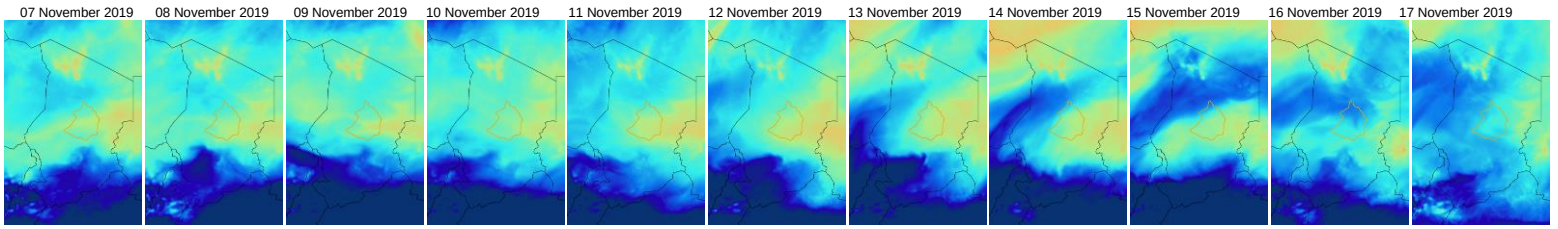

Fig.17 : Daily precipitations (NASA/GPM model)

0 mm/h 0.1 mm/h 2D_animation

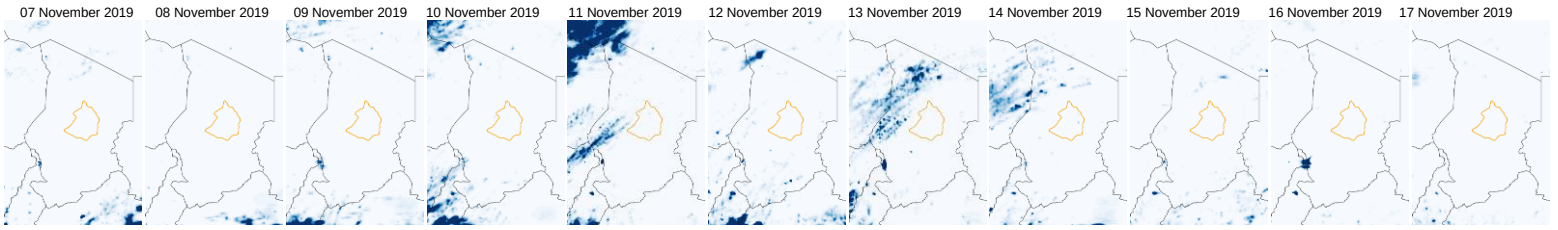

Fig.18 : Monthly precipitations since 2000 (NASA/GPM model).